Crustal motion along the Eurasia-Nubia plate boundary in the Calabrian Arc and Sicily and active extension in the Messina Straits from GPS measurements

Nicola D'Agostino and Giulio Selvaggi
Istituto Nazionale di Geofisica e Vulcanologia, Rome, Italy

Received 27 January 2004; revised 18 August 2004; accepted 26 August 2004; published 9 November 2004.

[1] We investigate crustal deformation along the Eurasia-Nubia plate boundary in Calabria and Sicily revealed by the GPS velocity field obtained by the combination of continuous site velocities with previous results from episodic campaigns. We recognize two distinct crustal domains characterized by different motions and styles of deformation. Convergence in Sicily is taken up by crustal shortening along the former Tyrrhenian back arc passive margin, in agreement with seismological data and geological evidence of recent cessation of deformation along the Plio-Pleistocene subduction front. The analysis of the GPS data and the consistency between earthquake slip vectors and convergence direction suggest that Eu-Nu convergence in Sicily does not require intermediate crustal blocks. Significant Eurasia (~3 mm/yr to NNE) and Nubia-fixed (~5 mm/yr to ESE) residual velocities in Calabria suggest instead the presence of an intermediate crustal block which can be interpreted as a forearc sliver or as an independent Ionian block. According to the first hypothesis, subduction is still active in the Ionian wedge, although we find no evidence for active back arc spreading in the Tyrrhenian Sea. The N115°E oriented Sicily-Calabria GPS relative motion is consistent with the extension observed during the 1908 M_w 7.1 Messina earthquake. We suggest that up to 3 mm/yr (~80%) of this estimated relative motion between Sicily and the Calabrian Arc may be taken up in the Messina Straits. *INDEX TERMS:* 1206 Geodesy and Gravity: Crustal movements—interplate (8155); 8102 Tectonophysics: Continental contractional orogenic belts; 8107 Tectonophysics: Continental neotectonics; 8158 Tectonophysics: Plate motions—present and recent (3040); *KEYWORDS:* active tectonics, GPS, Calabrian Arc, Messina Straits

Citation: D'Agostino, N., and G. Selvaggi (2004), Crustal motion along the Eurasia-Nubia plate boundary in the Calabrian Arc and Sicily and active extension in the Messina Straits from GPS measurements, *J. Geophys. Res.*, *109*, B11402, doi:10.1029/2004JB002998.

1. Introduction

[2] The M_w 7.1 earthquake that struck the Messina Straits on 28 December 1908, is one of the largest events [*Boschi et al.*, 1995] ever recorded in the central Mediterranean (Figure 1). Previous studies based on geodetic leveling, seismic waveforms inversion and long-term geological features have converged in the identification of a NNE-SSW trending active normal fault parallel to the strike and controlling the morphology of the Straits, as responsible for the 1908 earthquake [*Boschi et al.*, 1989; *Valensise and Pantosti*, 1992; *Pino et al.*, 2000; *Amoruso et al.*, 2002]. More controversial is the geodynamic framework in which active extension in the Messina Straits occurs. The evolution of this sector of the Eurasia-Africa plate boundary (Figure 1) over the Neogene and Quaternary times is generally interpreted in terms of slow relative plate convergence [*Argus et al.*, 1989; *DeMets et al.*, 1994] and fast subduction and roll-back of the Ionian lithosphere beneath the Calabrian Arc associated with back arc spreading in the Tyrrhenian Sea [*Malinverno and Ryan*, 1986; *Patacca et al.*, 1990; *Faccenna et al.*, 2001a]. For the understanding of the present-day pattern of deformation this model provides only limited insights because (1) direct geological and seismological evidence of active shortening in the Ionian Sea and contemporaneous back arc spreading in the Tyrrhenian Sea are lacking and (2) the position and direction of extension of the active fault in the Messina Straits, above the western edge of the Ionian slab, conflicts with its interpretation as a back arc extensional structure. The regional kinematic framework in which active extension in the Messina Straits occurs remains, therefore, poorly understood together with other issues such as (1) the influence of the Wadati-Benioff plane beneath the Tyrrhenian Sea on the crustal velocity field and (2) the distribution and style of active deformation along the plate boundary between Africa and Eurasia. Although geodetic studies aimed at monitoring crustal motion across the Messina Straits started as early as the 1970s, evidence of

0148-0227/04/2004JB002998$09.00

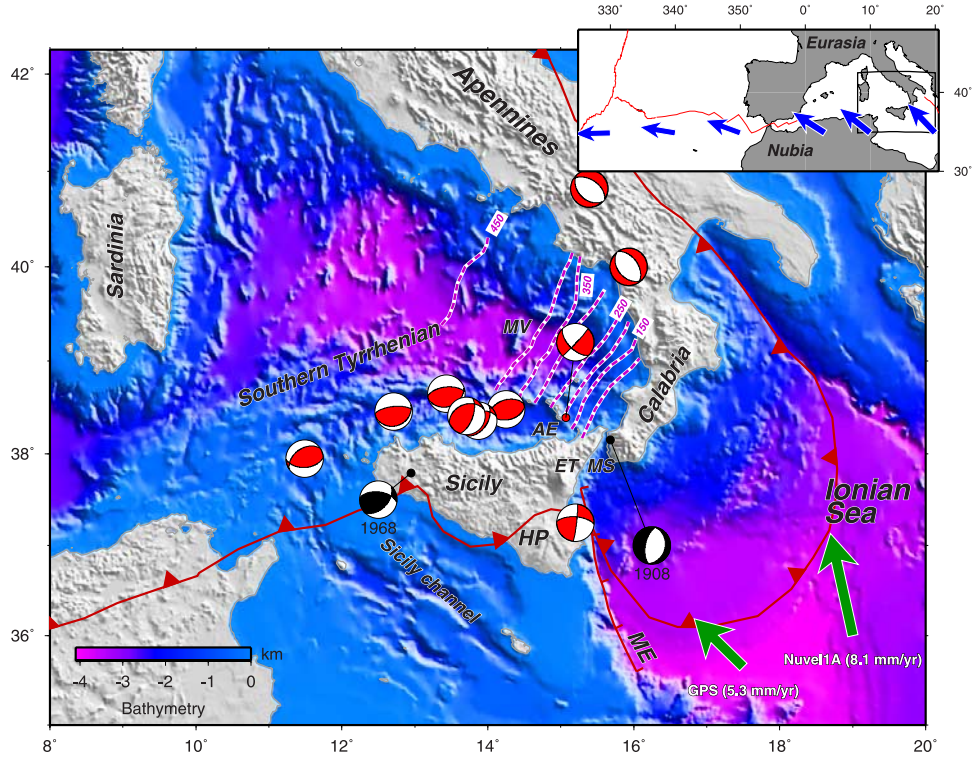

Figure 1. Regional tectonic map of the central Mediterranean area. Crustal focal mechanisms are selected from the CMT Catalog ($M_w > 5$, in red) and from *Anderson and Jackson* [1987] in black. The red lines show the trace of the Plio-Pleistocene subduction front (triangles) and Malta escarpment (ticks). Deep bathymetry marks the oceanic-floored Tyrrhenian (Neogene-Quaternary) and Ionian (Mesozoic) basins. Deep and intermediate seismicity in the Wadati-Benioff zone beneath the Tyrrhenian Sea, shown as contours of the subducted slab labeled in kilometers (modified from *Frepoli et al.* [1996]). Green arrows show the convergence vector between Nubia and Eurasia according to the Nuvel1A model and the GPS pole of rotation. The inset shows the convergence vectors along the Eurasia and Nubia plate predicted by the GPS Eu-Nu pole of rotation. Abbreviations are as follows: AE, Aeolian Islands; Et, Mount Etna; HP, Hyblean Plateau; ME, Malta escarpment; MS, Messina Strait; Mv, Marsili Volcano.

active extension based on trilateration and GPS across the Messina Straits have since remained elusive [*Anzidei et al.*, 1998].

[3] In this paper we use GPS data to estimate the crustal motion in the central Mediterranean plate boundary zone between the Eurasia and Nubia (e.g., the African plate west of the East African Rift) plates and propose a geodynamic framework for active extension in the Messina Straits. Inclusion of GPS continuous stations from the "stable" parts of the Eurasian and Nubian plates allows us (1) to define the kinematic boundary conditions imposed by the relative motion between the two plates and (2) to obtain site velocities in the deforming zone in both reference frames. We integrate our permanent site velocity solution with published denser survey-mode GPS results to obtain a combined velocity solution which allows us to estimate the active strain across the Messina Straits and discuss the implications for the regional seismic hazard.

2. Seismotectonic Setting

[4] The Calabrian Arc and the Sicily Island are located within the complex, articulated plate boundary between the Eurasian and African plates [*McKenzie*, 1972]. Figure 2 shows the instrumental seismicity recorded by the Italian National Seismic Network [*Chiarabba et al.*, 2004] in the period 1981–2003 and the events with hypocentral depths larger than 50 km extracted from the catalogue of relocated earthquakes of *Engdahl et al.* [1998] for the period 1964–1983. Beside the seismicity below the Etna volcano and along the Calabrian Arc, the most evident pattern of crustal seismicity is the east-west continuous belt north of Sicily in the Southern Tyrrhenian Sea showing thrust focal mechanisms with NNW-SSE and NW-SE compressive axes (Figure 1). The belt bends toward southeast in the proximity of the Aeolian Islands [*Pondrelli et al.*, 2004] where geological, geodetic, and seismological data [*Mazzuoli et al.*, 1995; *Bonaccorso*, 2002] suggest that the dominant deformation is right-lateral shear on NW-SE trending faults (Figure 1). Magnitude of the earthquakes along the E-W offshore seismic belt and in the Aeolian Islands has barely exceeded 5.5–6.0 during the instrumental period (the last being the M_w 5.7, 6/9/2002, Palermo earthquake). The region northeast of this continuous belt is dominated by the intermediate and deep events in the Southern Tyrrhenian Wadati-Benioff zone. Here, the depth distribution of earthquakes, as deep as 600 km, fairly well delineates the steeply (~70°) dipping Ionian lithosphere subducted beneath the

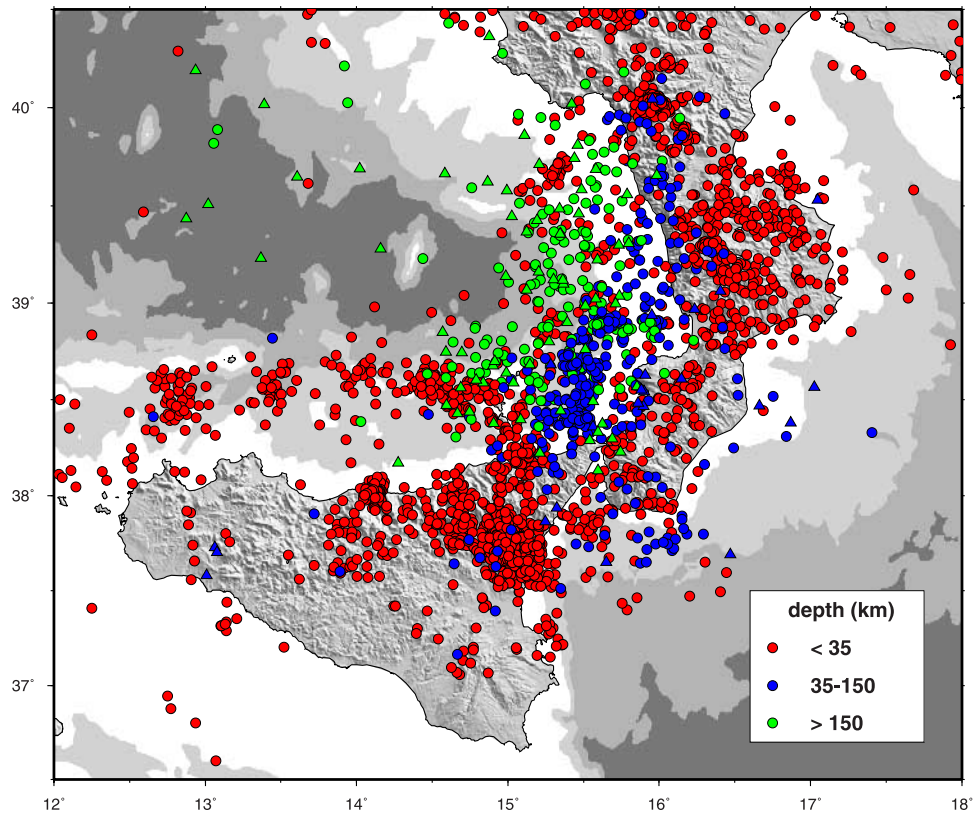

Figure 2. Seismicity map of Sicily and Calabria extracted from the catalog of earthquakes located by the Italian National Seismic Network [*Chiarabba et al.*, 2004] in the period 1984–2001 (circles) and from the catalog of relocated earthquakes (squares) with hypocentral depths larger than 50 km of *Engdahl et al.* [1998] for the period 1964–1984. The seismicity from the Italian National Network catalog is obtained merging arrival times of the National Network with those from local networks, increasing the spatial resolution and lowering the magnitude threshold for well located earthquakes (reported earthquakes have all errors within 4 km, at least 10 *P* wave arrival times, an azimuth gap below 200°, and RMS of the solution lower than 0.8 s). Crustal seismicity (depth <35 km) is especially concentrated along the Calabrian Arc, around the Etna volcano and in an E-W trending narrow belt north of Sicily. Deep and intermediate earthquakes seismicity, confined east of the Aeolian Islands, tracks the Ionian slab subducted beneath the Tyrrhenian Sea.

Calabrian Arc [*Selvaggi and Chiarabba*, 1995]. Fault plane solutions within the slab show pervasive downdip compression at all depths beneath 100 km, while at shallower depths downdip extension is observed [*Selvaggi*, 2001]. Deep and intermediate earthquakes in the Southern Tyrrhenian Wadati-Benioff zone abruptly terminates westward beneath eastern Sicily and the Aeolian Islands (Figure 2). The Hyblean Plateau shows a low level of instrumental seismicity in the past 20 years, although three destructive large earthquakes occurred in historical times in the years 1169, 1542 and 1693 A.D. [*Boschi et al.*, 1995]. The 1693 earthquake is probably one of the largest events that occurred in Italy with estimated magnitude of 7.2.

[5] The subduction of the Ionian lithosphere has been characterized during the Neogene and Quaternary by trench retreat and back arc extension, in response of the retrograde motion of the subduction hinge [*Malinverno and Ryan*, 1986]. Geological estimates of 50–70 mm/yr of back arc extension, averaged over the Neogene and Quaternary [*Patacca et al.*, 1990; *Faccenna et al.*, 2001a], provide significant evidence for vigorous trench retreat. Although direct seismological and geological evidence of the present-day subduction activity in terms of shortening in the accretionary wedge and spreading in the Tyrrhenian back arc basin are lacking, claims have been recently made for vigorous post-700 kyr trench retreat [*Gvirtzman and Nur*, 1999] and active plate divergence and lithosphere formation in the youngest part of the Tyrrhenian Sea, the Marsili seamount [*Marani and Trua*, 2002]. Active tectonics in Calabria and eastern Sicily is dominated by normal faulting along the Tyrrhenian side of Calabria and in the Messina Straits, describing a continuous extensional belt initially parallel (in Calabria) and subsequently cutting at high-angle (in the Messina Straits) across the front of the Apennine-Maghrebian thrust and fold-belt [*Tortorici et al.*, 1995]. In Sicily cessation of the active convergence along the Plio-Pleistocene nappe thrust front north of the Hyblean Plateau is suggested by Pleistocene deposits onlapping both the thrust front and the flexed north dipping foreland lithosphere in the Hyblean Plateau [*Butler et al.*, 1992; *Torelli et al.*, 1998]. The clear contractional character of the active deformation in the Southern Tyrrhenian Sea

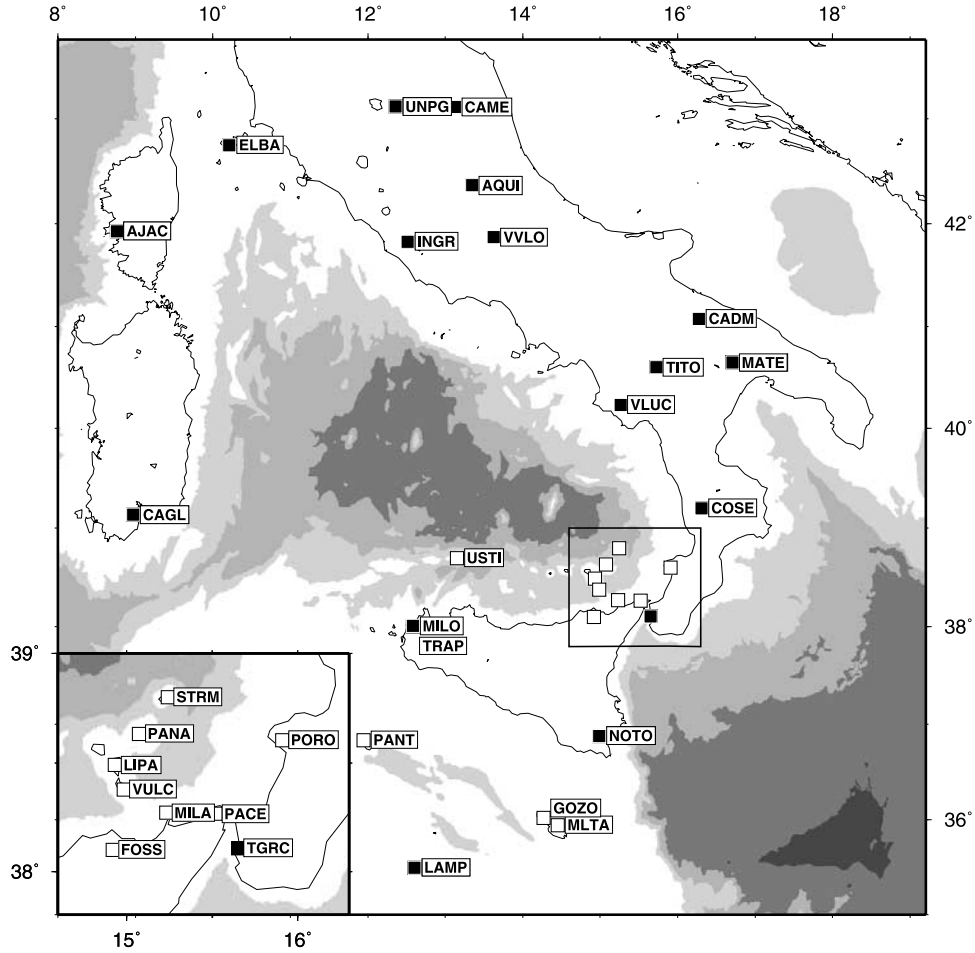

Figure 3. GPS site distribution. Solid boxes represent continuous GPS stations, whereas open boxes are campaign-mode GPS sites from *Hollenstein et al.* [2003].

(Figure 1), contrasts with late Pliocene-early Pleistocene normal fault growth and subsiding basins, imaged in offshore seismic lines [*Pepe et al.*, 2000]. These extensional structures represent the southern boundary of the Tyrrhenian extensional back arc domain. Thrust fault plane solutions and the lack of clear evidence of inverted structures on the seismic lines [*Pepe et al.*, 2000] imply that a recent tectonic change in the tectonic regime may have occurred along this margin in relation to the cessation of activity along the thrust front north of the Hyblean Plateau and northward migration of the locus where the Eu-Nu convergence is accommodated. It is not clear whether the thrust fault earthquakes reactivate preexisting north dipping extensional faults, related to the Tyrrhenian back arc extension, or rupture south dipping faults accommodating the overthrusting to the north of the Sicilian continental block over the thinned Tyrrhenian crust.

3. Data Analysis

3.1. Continuous GPS Measurements (CGPS)

[6] Continuous GPS measurements were analyzed using the GIPSY software developed at the Jet Propulsion Laboratory. Nonfiducial satellite orbits, clock files and transformation parameters from free-network to ITRF2000 were imported from JPL (ftp://sideshow.jpl.nasa.gov). In order to define the velocity field with respect to the Eurasian and Nubia plates, we included in our analysis stations located on the stable parts of these plates. In a first processing step daily solutions in the ITRF2000 reference frame for individual station position and corresponding matrices of the covariance among the three position components, spanning the time interval 1996.0 to 2004.5, were initially determined using a precise point positioning strategy [*Zumberge et al.*, 1997]. We then obtained a "regional" ITRF2000 velocity solution for selected stations with the longest observation interval and minimum antenna-receiver operations (ZIMM, GRAS, GRAZ, TORI, GENO, CAGL, MATE, and NOTO), by least squares fitting their weekly averaged Cartesian positions. In the following step, sites located within the area of interest (Figure 3) were brought together for local-network processing and ambiguity resolution. The free-network ambiguity-fixed daily solutions were then transformed into the ITRF2000 by estimating a seven-parameter similarity transformation for each. We estimated the transformation for each day, on the basis of selected common stations that are present both in the ITRF2000 "regional" solution and in the daily ambiguity-fixed solution. On average seven common stations were present both in the ambiguity-fixed and "regional ITRF2000" solution (a minimum of three common stations were required to evaluate daily transformation parameters). From the ITRF2000 daily

positions rotated in a local NEU frame we simultaneously estimated, with a weighted least squares approach for each station, a linear station velocity, an annual, and a semiannual periodic signal. Antenna offsets were estimated at discontinuities in the time series related to known equipment change or where a clear discontinuity was observed in the time series. Only time series with an interval longer than 2.5 years have been considered for velocity estimation to mitigate the effect of the bias introduced by a periodic annual signal [*Blewitt and Lavallée*, 2002]. Only the PHLW site with a slightly shorter time series was retained for its interest. The velocity uncertainties presented in this paper for CGPS measurements account for both noncorrelated (white noise) and temporally correlated site positions effects. We adopted a simple empirical model for estimating the GPS rate error [*Mao et al.*, 1999; *Dixon et al.*, 2000] that includes white and flicker noise. Weighted root mean squared from time series of position for individual stations was used to scale these contributing processes. Using ITRF2000 site velocities (Table 1) and associated errors we estimated the Euler poles of rotation for both the Eurasian and Nubia plates by minimizing, with a weighted least squares inversion, the adjustments to horizontal velocities of 26 stations within the stable Eurasia and 10 stations within the stable Nubia (Tables 2 and 3). The RMS of residuals and the fitting procedure result in a reduced chi-square of about 1 indicating that a rigid plate is an adequate approximation given the uncertainties in the GPS velocities. The relative Eu-Nu pole of rotation (Figure 4) is then derived by differencing the ITRF2000 angular velocities with appropriate error propagation. The convergence vector derived by our GPS Eu-Nu pole of rotation (5 ± 0.28 mm/yr to N45W ± 3° at 17.50°E, 36.65°N) significantly differs from the prediction obtained by the closure of the Africa-North America-Eurasia plate motion circuit [*Argus et al.*, 1989; *Calais et al.*, 2003]. Our solution displays (Figure 1) a 35% smaller and 30° more westerly directed convergence direction in Calabria and Sicily, similarly to others recently published GPS Eu-Nu poles of rotation [*Sella et al.*, 2002; *McClusky et al.*, 2003; *Fernandes et al.*, 2003; *Calais et al.*, 2003]. Whether this discrepancy reflects a real change in Nubia-Eurasia plate motion or unrecognized systematic errors in both geodetic and geological data is discussed in detail by *Calais et al.* [2003] and will not be discussed here, since the Eu-Nu GPS pole of rotation derived in the present study and in the former quoted papers are similar and not statistically different at the 95% confidence interval.

3.2. Combination With Episodic GPS Measurements

[7] A recent study by *Hollenstein et al.* [2003] presents the results of periodic GPS surveys in southern Italy and provides supplemental data to integrate our permanent sites velocity solution. The distribution of the geodetic sites (Figure 3) analyzed by *Hollenstein et al.* [2003] allows us to obtain a dense station coverage in those parts of Sicily and neighboring islands not covered by permanent stations and one more site in Calabria (PORO). Site velocities were estimated by *Hollenstein et al.* [2003] in the ITRF97 reference frame and then rotated in a Eurasia reference using the ITRF97-Eurasia REVEL pole of rotation of *Sella et al.* [2002]. Our permanent sites (Figure 5) and the survey sites velocity solutions are thus nominally in the same Eurasian reference frame, but minor discrepancies are shown at common stations, producing an RMS of the differences in east and north velocities of 0.48 and 0.71 mm/yr. We minimized these discrepancies by inverting with a weighted least-square algorithm, for the rigid rotation that minimizes the differences in velocity at common stations (CAGL, NOTO, MATE, UNPG, LAMP) using the CGPS velocities as the reference solution. The RMS of the velocity differences after combination is reduced to 0.18 and 0.23 mm/yr in the eastern and northern directions, respectively. The nearby MILO and TRAP sites (which were not used to estimate the rigid-rotation parameters) permit to evaluate the consistency between the CGPS and episodic velocities data sets (Figure 6). The ~2 mm/yr difference is not statistically significant at the 95% confidence interval. The factors which may contribute to this difference may include the relatively long time interval covered by the survey-style measurements of TRAP (7 years) compared with the short time interval of CGPS measurements (2.8 years) at MILO which may still be contaminated by periodic signal.

4. Combined GPS Velocity Field

[8] Figure 6 shows the combined GPS velocity field in the Eurasian and Nubia reference frames. GPS sites lying on one of the two stable plates within 95% confidence interval are CAGL and AJAC, lying on the Eurasian plate, and LAMP lying on the Nubia plate. The velocity of NOTO site, previously considered to lie on the African plate [*Ward*, 1994], is similar to the motion of Nubia but shows a small but significant 2 mm/yr residual toward N77°E that may be explained either by active extension in the Sicily channel or by elastic strain accumulation on nearby active faults. The last hypothesis, supported by the severe damage (I > X MCS) suffered during the 1693 M 7.2 earthquake [*Boschi et al.*, 1995], still considers southern Sicily and NOTO as lying on the Nubia plate, but allows some minor contamination of the NOTO velocity by elastic strain accumulation on a still poorly documented N-S off-shore active fault along the Malta escarpment. A similar fault geometry has been used by *Piatanesi and Tinti* [1998] to model the tsunami of the 1693 earthquake. The small Nubia-fixed residuals of NOTO and LAMP, the small velocity gradients between NOTO and TRAP, the significant velocity gradient between TRAP and USTI together with the continuous band of seismicity in the Southern Tyrrhenian, all suggest that the Nubia motion is partly transferred across western and southern Sicily and absorbed by shortening in the Southern Tyrrhenian at a rate of ~4 mm/yr. This observation argue for accommodation of the Eu-Nu convergence somewhere between Sardinia to the north and the Hyblean Plateau and Sicily channel to the south in agreement with seismological and geological evidence of recent cessation of activity along the subduction front in mainland Sicily. On the basis of a smaller number of CGPS sites, *McClusky et al.* [2003] reached a similar interpretation placing the Nubia-Eurasia boundary north of station NOTO and south of Sardinia.

[9] In Calabria the two permanent sites COSE and TGRC, and the survey site PORO, have similar velocities of ~5 mm/yr to ESE (Nubia-fixed), and ~3 mm/yr to NNE (Eurasia-fixed). This pattern shows that Calabria has an

Table 1. GPS Site Positions, Velocities, 1-Sigma Uncertainties, Correlation Between the East and North Components of Velocity, Time Span, Number of Observing Days, and Residual Velocities[a]

			ITRF2000 Velocity, mm/yr							Residual, mm/yr	
Site	Longitude, °E	Latitude, °N	East	North	E(±)	N(±)	corr	ΔT	ntot	East	North
					Eurasia[b]						
ARTU	58.560	56.430	24.97	5.08	0.39	0.43	0.08	4.65	1650	−0.14	−0.64
BOGO	21.035	52.476	21.49	14.03	0.33	0.38	0.15	5.95	2096	0.80	0.60
BOR1	17.073	52.277	19.59	13.81	0.28	0.31	0.04	8.25	2960	−0.40	−0.15
BRST	355.503	48.380	15.62	16.26	0.74	0.56	−0.04	5.25	1507	−1.08	0.65
BRUS	4.359	50.798	17.75	14.63	0.27	0.56	−0.12	8.25	2948	−0.08	−0.56
CASC	350.582	38.693	17.28	16.02	0.58	0.48	−0.01	4.99	1634	−1.10	0.34
CRAO	33.991	44.413	24.28	11.81	0.86	0.67	0.04	3.91	1216	−0.06	0.54
GLSV	30.497	50.364	22.21	12.07	0.34	0.28	0.19	6.09	2131	−0.57	0.16
GOPE	14.786	49.914	19.88	13.66	0.32	0.29	−0.01	8.25	2925	−0.24	−0.57
JOZE	21.032	52.097	20.95	13.45	0.29	0.37	0.03	8.25	2958	0.17	0.02
KIT3	66.885	39.135	27.57	3.75	0.45	0.38	−0.09	9.49	2021	−0.19	0.21
LAMA	20.670	53.892	20.18	13.32	0.33	0.40	−0.01	8.25	2802	−0.10	−0.16
MDVO	37.224	56.028	22.87	10.82	0.47	0.50	0.13	7.07	2468	0.23	0.18
MOBN	36.569	55.115	22.54	10.76	0.73	0.66	0.03	3.01	1086	−0.20	−0.01
MOPI	17.274	48.373	20.86	14.85	0.44	0.47	−0.02	5.97	2149	−0.07	0.92
PENC	19.282	47.790	22.10	13.70	0.30	0.36	0.07	7.61	2607	0.68	0.03
POLV	34.543	49.603	22.82	11.00	0.59	0.64	0.10	2.78	981	−0.73	−0.17
POTS	13.066	52.379	19.13	14.51	0.28	0.30	0.00	8.25	2928	−0.05	0.09
PTBB	10.460	52.296	19.56	15.35	0.47	0.51	0.05	4.00	1347	0.88	0.66
TIXI	128.867	71.635	17.07	−12.15	0.41	0.44	0.02	5.47	1900	−0.10	−0.33
UZHL	22.298	48.632	21.52	12.98	0.46	0.47	0.08	4.74	1528	−0.25	−0.27
VILL	356.048	40.444	18.69	15.77	0.39	0.65	−0.01	9.22	3131	−0.20	0.18
WROC	17.062	51.113	20.21	13.21	0.33	0.32	−0.01	7.09	1987	−0.06	−0.75
WTZR	12.879	49.144	20.32	14.87	0.36	0.33	−0.06	8.22	2961	0.38	0.43
ZECK	41.565	43.788	25.36	10.36	0.40	0.36	0.03	6.14	1967	−0.02	0.62
ZWEN	36.759	55.699	23.43	10.82	0.45	0.45	0.16	8.25	2425	0.79	0.09
					Nubia[b]						
GOUG	350.119	−40.349	18.93	17.42	1.46	0.75	0.09	5.63	1722	−0.40	0.06
HARB	27.707	−25.887	15.68	16.35	0.95	0.71	−0.05	3.32	1119	−0.49	−0.37
HRAO	27.687	−25.890	16.37	16.55	0.56	0.39	−0.05	7.00	2228	0.20	−0.17
MAS1	344.367	27.764	15.31	16.99	0.50	0.37	−0.11	7.24	2383	−0.43	0.20
NKLG	9.672	0.354	21.34	17.90	1.15	0.64	0.00	4.00	1409	0.13	−0.09
PHLW	31.343	29.861	22.72	17.42	1.25	1.01	0.10	2.39	778	0.44	1.16
RABT	353.146	33.998	16.40	16.87	0.96	0.59	0.11	3.87	1280	0.97	−0.72
SIMO	18.440	−34.188	13.55	17.48	1.51	1.36	−0.16	2.55	783	−1.81	−0.11
SUTH	20.811	−32.380	16.53	17.68	0.82	0.48	−0.07	5.96	2040	1.09	0.27
TGCV	337.017	16.755	19.49	16.03	1.23	1.29	−0.18	3.56	159	1.66	0.22
					Plate Boundary[c]						
AJAC	8.763	41.928	20.74	14.90	0.22	0.26	−0.10	4.51	1463	−0.05	0.06
AQUI	13.350	42.368	20.28	16.01	0.25	0.32	0.35	5.11	1771	−1.20	1.62
CADM	16.274	41.078	23.99	18.52	0.38	0.44	0.13	3.18	583	1.79	4.46
CAGL	8.973	39.136	21.20	14.96	0.10	0.14	−0.09	8.39	2733	−0.17	0.13
CAME	13.124	43.112	22.55	17.40	0.31	0.47	0.03	4.24	1348	1.25	2.98
COSE	16.310	39.201	23.38	17.25	0.37	0.37	0.09	4.24	700	0.86	3.20
ELBA	10.211	42.753	20.14	15.33	0.28	0.37	−0.16	3.71	1299	−0.73	0.62
GENO	8.921	44.419	19.99	15.13	0.12	0.18	−0.04	6.00	2084	−0.30	0.30
GRAS	6.921	43.755	19.72	15.45	0.09	0.13	0.00	8.56	2669	−0.35	0.45
GRAZ	15.493	47.067	21.65	15.27	0.10	0.18	0.03	8.08	2726	0.75	1.12
INGR	12.515	41.828	21.30	16.63	0.25	0.28	0.07	4.16	1357	−0.15	2.15
LAMP	12.606	35.500	19.47	17.71	0.16	0.17	0.02	5.27	1786	−3.07	3.24
MATE	16.704	40.649	23.19	18.53	0.09	0.13	0.06	8.56	2833	0.84	4.53
MILO	12.584	38.008	20.84	17.84	0.62	0.66	−0.04	2.80	888	−1.30	3.37
NOTO[d]	14.990	36.876	20.72	18.70	0.17	0.13	0.03	8.56	2929	−1.97	4.49
TGRC	15.651	38.108	23.79	17.07	0.41	0.40	−0.08	4.02	1059	1.19	2.94
TITO	15.724	40.601	22.53	17.97	0.44	0.46	0.02	3.45	917	0.33	3.85
TORI	7.661	45.063	19.91	15.17	0.11	0.15	−0.04	7.31	2421	0.00	0.23
UNPG	12.356	43.119	20.62	16.35	0.20	0.20	0.04	6.19	2054	−0.55	1.85
VLUC	15.266	40.231	21.72	16.43	0.30	0.30	0.01	4.89	1007	−0.47	2.25
VVLO	13.623	41.870	22.11	17.26	0.36	0.47	0.32	4.05	1233	0.49	2.90
ZIMM	7.465	46.877	19.41	14.89	0.10	0.13	0.01	7.86	2686	−0.04	−0.07

[a]Definitions are as follows: ΔT, time span; ntot, number of observing days; corr, correlation; E(±) and N(±), 1-sigma uncertainties.
[b]Residual velocities are relative to the respective plate.
[c]Residual velocities in the plate boundary are relative to Eurasia.
[d]NOTO velocity is obtained from the composite time series of NOTO prior to 6 September 2000, and NOT1 thereafter.

Table 2. Plate Angular Velocities in Geographic Coordinates

Plate	Latitude, °N	Longitude, °E	ω[a]	σ_{maj}[b]	σ_{min}[b]	Azim[c]	σ_ω[d]	N. Sites[e]	$\chi\nu^2$[f]	RMS East[g]	RMS North[g]
Eu(ITRF2000)	56.105	−100.064	0.253	1.0	0.3	35.4	0.002	26	1.27	0.50	0.44
Nu(ITRF2000)	49.624	−84.259	0.250	1.0	0.6	88.3	0.002	10	0.70	0.95	0.47
Nu-Eu[h]	−22.463	−28.772	0.050	6.8	3.4	30.5	0.003				

[a]Parameter ω is the rotation rate in deg/Myr.
[b]Two-dimensional 1-sigma lengths in degrees of the semimajor σ_{maj} and semiminor axes σ_{min} of the pole error ellipse.
[c]Azimuth of the semimajor ellipse axis in degrees clockwise from north.
[d]One-sigma error of the rotation rate in deg/Myr.
[e]Number of sites used to estimate the pole of rotation.
[f]The parameter χ^2 per degree of freedom.
[g]Root-mean-square of the rate residual, north and east components in mm/yr.
[h]First plate rotates counterclockwise with respect to the second plate around the listed rotation pole.

independent motion with respect to both the Eurasia and Nubia plates. Two hypotheses can be proposed. (1) Assuming that the Ionian lithosphere is attached to the south to the Nubian lithosphere and considering that CAGL and AJAC have very small Eurasia-fixed velocities (i.e., they lie on the overriding plate of the Calabrian subduction), the Nubia-fixed velocities can be used to evaluate the subduction rate of the Ionian lithosphere beneath Calabria whereas the Eurasia-fixed velocities can be used to evaluate the rate of back arc extension in the Tyrrhenian Sea. The eastward directed Nubia-fixed velocities suggest that convergence between Calabria and Nubia is absorbed in the Ionian submerged wedge by the underthrusting of the Ionian lithosphere beneath Calabria. The insignificant elongation of the baselines between the Calabrian Arc (TGRC, PORO, COSE) and the Sardinia-Corsica block (AJAC-CAGL) shows, on the other hand, that although subduction may still be active, the Tyrrhenian basin is not actively spreading. Our results thus do not support recent claims of active plate divergence in the most recent part of the Tyrrhenian basin, the Marsili seamount [*Marani and Trua*, 2002] and vigorous trench retreat [*Gvirtzman and Nur*, 1999], which is generally associated with active back arc extension. (2) If, alternatively, the Ionian lithosphere is not part of Nubia, the GPS velocities in the Calabrian Arc are probably representative of deformation and strain accumulation at the margins of a rigid block located in the Ionian Sea (a more complete discussion is given in section 6.1).

[10] The combined velocity solution shows significant N-S velocity gradient between NOTO and the sites in northeastern Sicily (Figure 6b), resulting in a northward acceleration and an approximately N-S directed extension. The sites located at the extreme northeastern corner of Sicily, move toward NE with respect to Sicily, perpendicularly to the Eu-Nu convergence, and progressively rotate from NE to ESE above the western edge of the Ionian slab (Figure 6b) where deep and intermediate earthquakes track the slab at a depth between 100 and 250 km (Figure 2). Geodetic velocities projected along N30°E (Figure 7) show decreasing values from Sicily to the Aeolian Islands and statistically constant values along the Calabrian Arc. These observations are consistent with (1) buttressing of northeastern Sicily and the Aeolian Islands against the Tyrrhenian basin, and (2) rigid motion of the Calabrian block toward NE. How the motion of the Calabrian Arc toward NE is related to the kinematics of the Adria microplate and the Apulian block is not clear but increasing velocities of MATE and CADM suggest that the Apulian block does not buttress the Calabrian Arc.

[11] Active extension across the Apennines at 3 mm/yr is shown by the increasing velocities between the Tyrrhenian site (VLUC) and the Adriatic sites (MATE, CADM) and confirms early hypotheses based on GPS reoccupation of the first-order triangulation network [*Hunstad et al.*, 2003], and episodic campaigns [*Anzidei et al.*, 2001]. Both Eurasia

Table 3. Covariance Matrix of the Angular Velocities in Cartesian Coordinates

Plate	xx[a]	xy[a]	xz[a]	yy[a]	yz[a]	zz[a]
Eu(ITRF2000)	1.261	0.462	0.462	0.404	0.646	2.290
Nu(ITRF2000)	2.769	0.311	0.311	0.696	−0.046	1.574
Nu-Eu	4.030	0.773	0.773	1.100	0.600	3.864

[a]These six columns give the elements of the covariance matrix (10^{-9} rads^2/Myr^2).

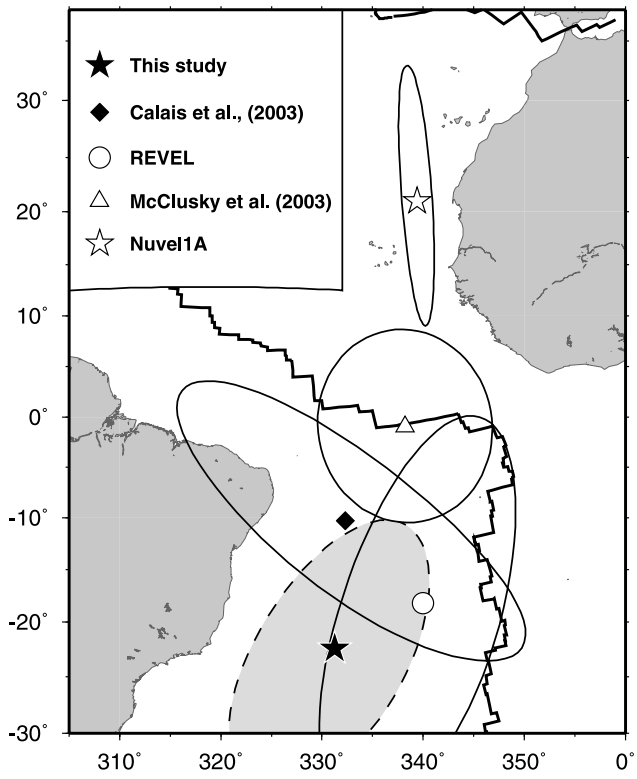

Figure 4. Eurasia-Nubia Euler poles of rotation derived in this and previous studies. REVEL pole is taken from *Sella et al.* [2002]. Nuvel1-A is taken from *DeMets et al.* [1994]. Uncertainty ellipses show 95% confidence limits.

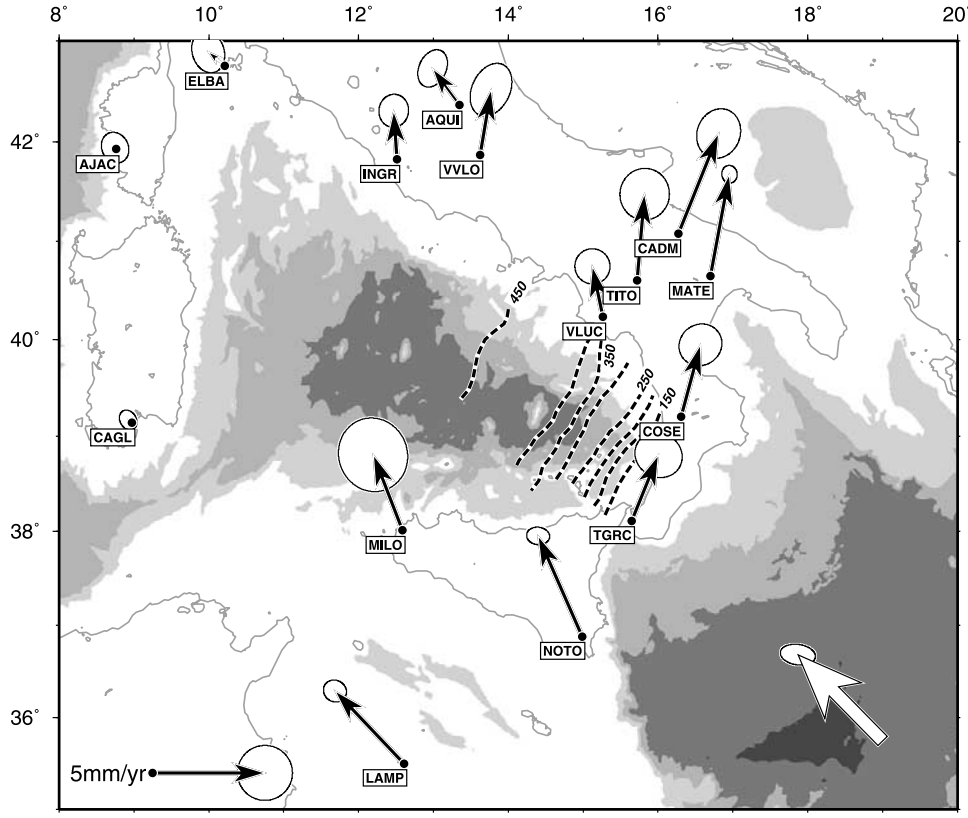

Figure 5. GPS velocities of continuous sites and 95% confidence ellipses in a Eurasia reference frames. The large white arrow in the Ionian Sea is the convergence vector predicted by the GPS-derived Eu-Nu Euler pole. Confidence ellipses are computed by adding the variance of the rotation vector defining the reference frame to the variance of the site velocities.

and Nubia fixed velocities display significant residuals, arguing for an independent Adriatic microplate [*Anderson and Jackson*, 1987; *McClusky et al.*, 2003], although the definition of internal rigidity and location of its southern boundary is still a matter of debate [*Oldow et al.*, 2002; *Calais et al.*, 2002; *Battaglia et al.*, 2004] and outside the scope of this paper.

[12] If Calabria and Sicily are characterized by different crustal motions it is important to define the style and kinematics along their common boundary with the aim of characterizing and quantifying the strains that might be released in large earthquakes. Since the site velocities in Calabria are not statistically different, we assume that TGRC is not significantly affected by interseismic elastic effects and postseismic transients after the 1908 Messina earthquake and can be considered as representative for the motion of the Calabria Arc. If we further assume that NOTO is representative of the motion of the southern and western Sicily, we can use a velocity diagram to obtain an estimate of the relative motion between Sicily and Calabria (Figure 8). Because this estimate relies on only two sites, the results of this simple calculation should be considered as a first-order estimate before more complete geodetic data are available. The diagram shows a relative TGRC-NOTO motion of 3.6 ± 06 mm/yr to N115°E ± 7°, approximately perpendicular to the strike of the Messina Strait fault and close to the slip vector of the 1908 Messina earthquake [*Boschi et al.*, 1989]. The results of this simple analysis thus suggest that the direction of crustal extension from geological data and from the slip vector of the 1908 Messina earthquake are consistent with the relative motion between Sicily and Calabria and provide a preliminary upper bound on the total extension taken up in the Messina Straits. In the next section the combined velocity solution will be used to characterize the pattern of active deformation between Sicily and Calabria and evaluate the rate of strain accumulation in the Messina Straits.

5. Strain Rate Analysis and Active Extension in the Messina Straits

[13] From the combined velocity solution we proceed to evaluate the strain and rigid-rotation field in the boundary zone between the Calabrian Arc and Sicily (Figure 9). We have made discrete estimates of the velocity gradient tensor at points on a 30 km regular grid, using the velocities of a minimum of four sites. If only three such sites exist we do not compute a velocity gradient tensor because such an estimate, being even determined, is liable to instability, particularly if two of the three sites are much closer to each other than to the third. The covariance matrix used to estimate the velocity gradient tensor starting from site velocities is a weighted version of the velocity covariance matrix where the weighting factor [*Shen et al.*, 1996] is $\exp(2 * d^2/s^2)$, where d is the distance of the geodetic site to the point to be estimated and s is a distance-decaying constant, taken as 60 km. This weighting means that a station at 50 km away from the spot to be evaluated will

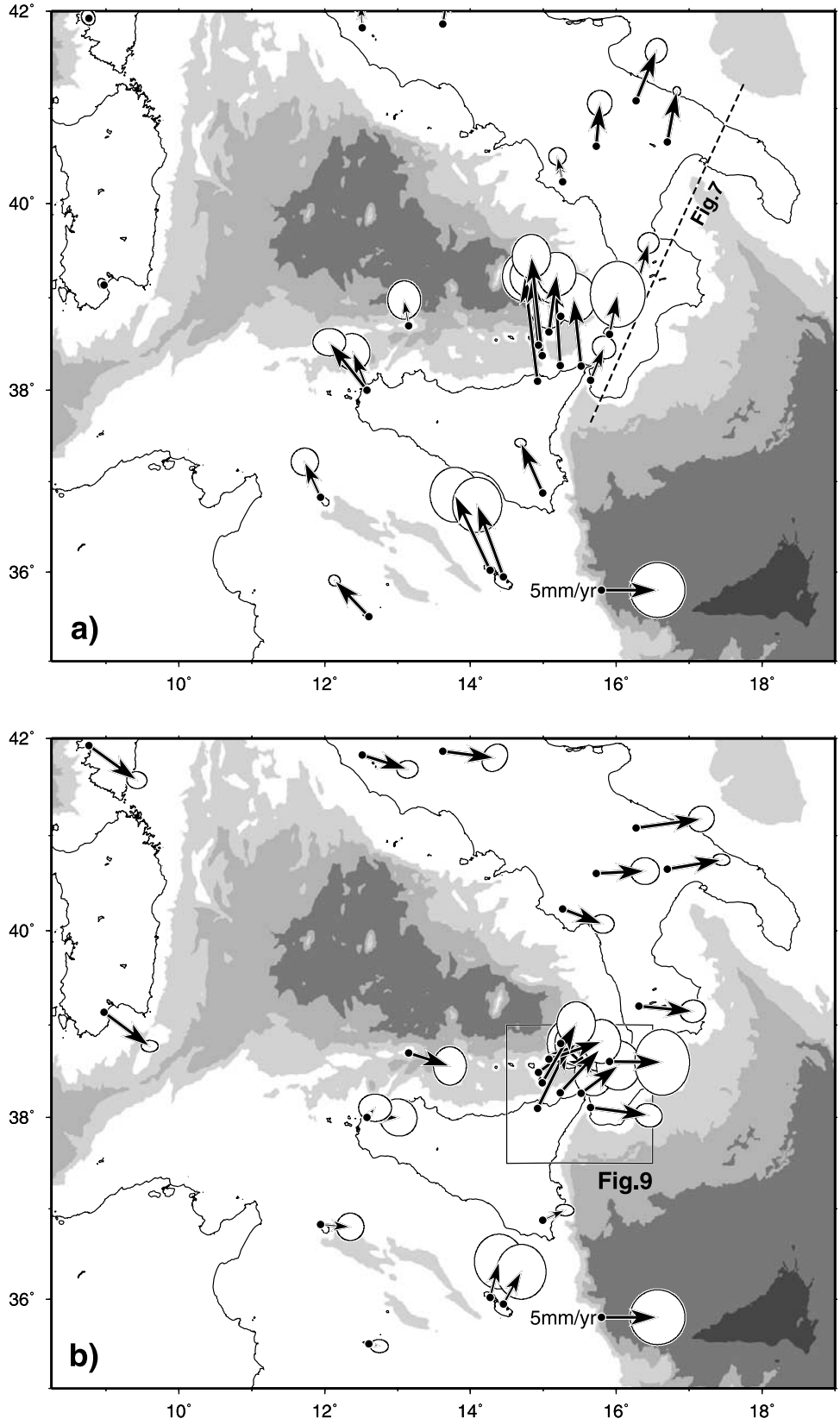

Figure 6. GPS velocity fields in the (a) Eurasia and (b) Nubia reference frames obtained by combining the permanent sites velocity solution with the results of survey sites solution of *Hollenstein et al.* [2003].

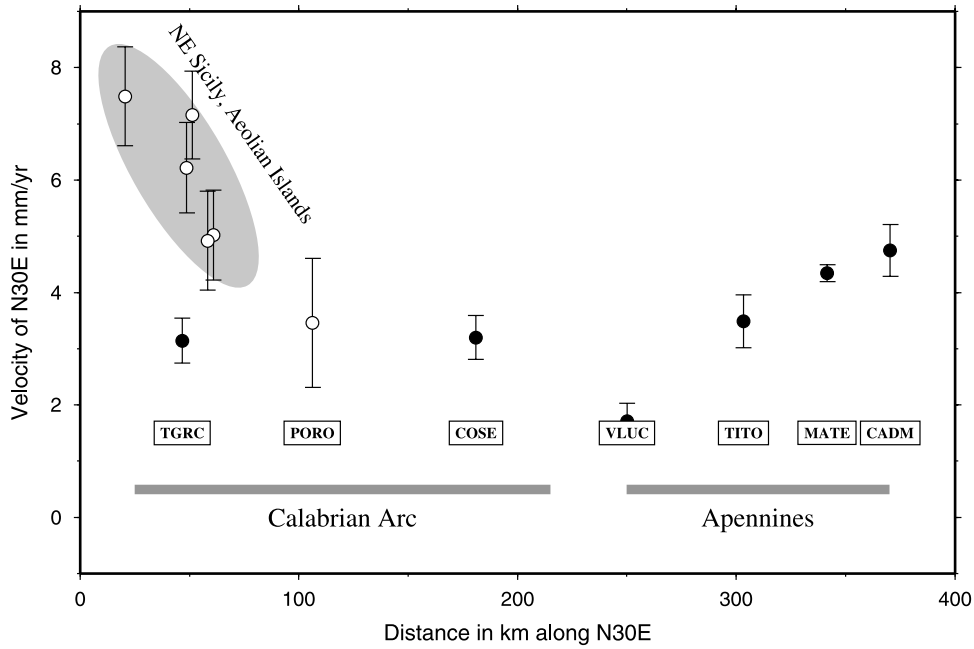

Figure 7. Velocity in the N30°E direction as a function of distance along the same direction for permanent (solid circles) and survey mode sites (open circles). The error bars represent 1 standard deviation. Decreasing velocities in the Aeolian Islands and in northeastern Sicily suggest buttressing of this region against the Tyrrhenian crust behind the Calabrian Arc. Similar rates of NE motion in the Calabrian Arc and increase in velocity toward the Apulian block (MATE, CADM) suggest that this region is rigidly translating to NNE and that its motion is not buttressed by the Apulian block. Active extension of about 3 mm/yr is observed across the Apennines.

contribute only one-half its unweighted value to the velocity solution. The advantage of this algorithm is that strain rate estimates are less biased because of proper weighting and they are stable because they are evaluated weighted averages over the region. The geodetic sites at Stromboli (STRM) and Panarea (PANA) have not been considered because suspected of being contaminated by local magmatic deformation that culminated in the volcanic activity of December 2002. The area is characterized by rapid variation of the principal axes of the strain rate tensor changing from NNE trending compressional strain rates in the Aeolian Islands (∼50 nanostrain/year) to SE extensional strain rates in the Messina Straits (∼100 nanostrain/year). An homogeneous pattern of instantaneous rotation rates of about 2°–3°/Myr characterizes the area under study. The strain distribution is in agreement with geological observation pointing for NW right-lateral strike slip in the Aeolian Islands [*Mazzuoli et al.*, 1995] and WNW-ESE directed extension in the Messina Straits [*Valensise and Pantosti*, 1992], and with the focal mechanisms of the largest earthquakes in the area (Figure 9a).

[14] Beyond a simple comparison between the distribution of strain rates and geological and seismological observations, we can ask what pattern of uniform faulting (e.g., the single set of parallel faults) can accommodate the observed velocity field. *Holt and Haines* [1993] show that within a three-dimensional strain rate field, in which the magnitude of shear strain rates exceeds the magnitude of dilatational strain rate, there are two possible strike directions of faulting that can produce the horizontal components of the strain rate tensor. These are directions of zero length change in the

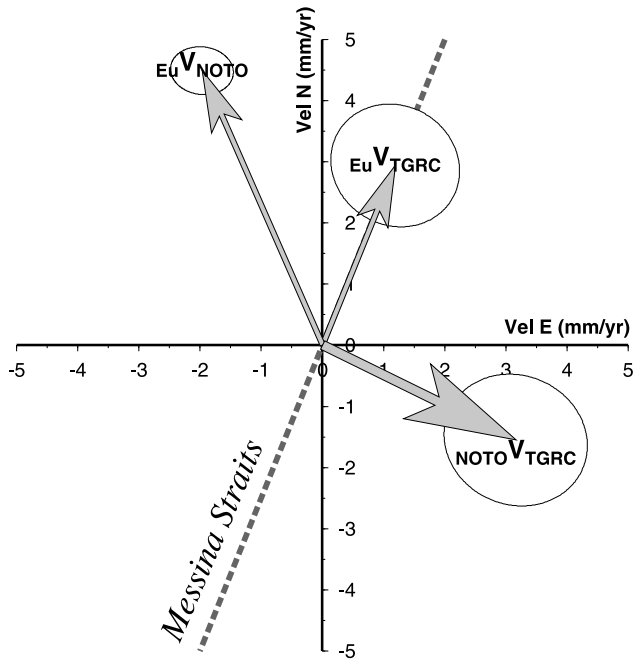

Figure 8. Velocity diagram showing the relative motion between Calabria (site TGRC) and Sicily (site NOTO) that in our interpretation can be considered as distinct crustal blocks. The relative velocity vector ($_{NOTO}V_{TGRC}$) is consistent with 3.6 ± 06 mm/yr of N115°E relative motion between the two blocks roughly perpendicular to the trend of the Messina Straits (N25°E, shown as a thick gray dashed line).

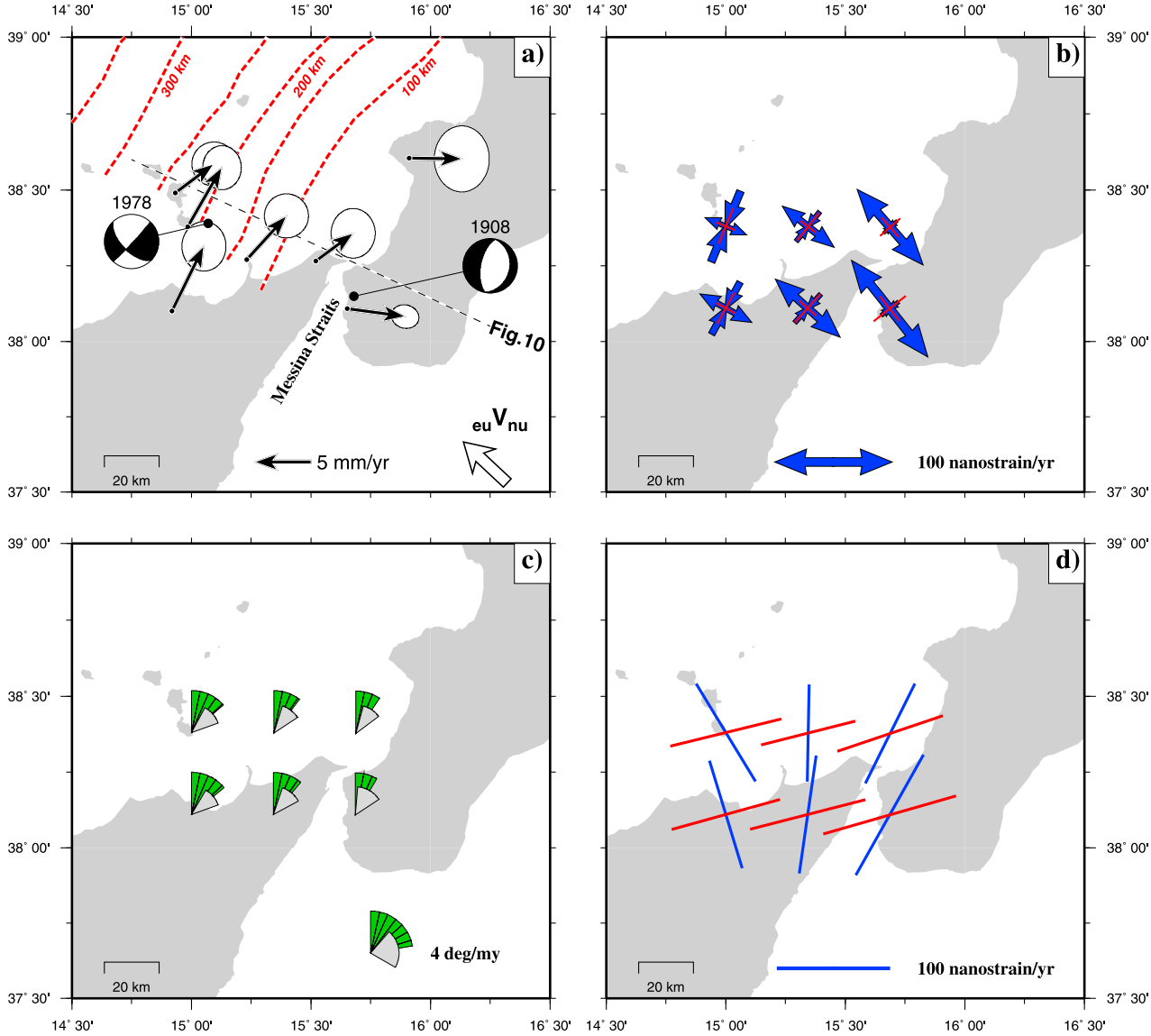

Figure 9. (a) Combined velocity solution in a Nubia reference frames. Focal mechanisms of the 1908 M_w 7.1 Messina earthquake and 1978 M_w 6.0 Golfo di Patti earthquake are also shown together with the depth contours of the Ionian slab. The thin dashed line indicates the section used to project site velocities shown in the velocity diagram in Figure 10. (b) Principal axes of the horizontal strain rate tensor (in blue) and associated 1 sigma errors (red bars). (c) Rotation rates (green wedges and associated 1 sigma error in gray) on a 30 km regular grid (more details in the text). (d) The orientation of uniform faulting that can accommodate the strain rate field shown in Figure 9b. Red lines are faults with a left-lateral component; blue lines are faults with a right-lateral component. Line lengths are equal to the magnitude of the difference between the principal strain rates. Observe the consistency with the observed NW direction of right-lateral faulting in the Aeolian Islands and with the fault-controlled direction of the western side of the Messina Straits.

velocity field, and they correspond to the strikes of the two nodal planes in a fault plane solution. In terms of the elements of the strain rate tensor, these strikes are

$$\tan\theta = \frac{-\dot{\varepsilon}_{xy} \pm \sqrt{\dot{\varepsilon}_{xy}^2 - \dot{\varepsilon}_{xx}\dot{\varepsilon}_{yy}}}{\dot{\varepsilon}_{yy}}, \qquad (1)$$

where $\dot{\varepsilon}_{xy}$, $\dot{\varepsilon}_{xx}$, $\dot{\varepsilon}_{yy}$ are the three horizontal strain rate tensor components and θ is the strike angle of the fault measured anticlockwise from the x (east) axis. In Figure 9d we plot the strike directions of planes of shear (zero length change) derived from the components of the strain rate tensors shown in Figure 9b. The lengths of the lines shown in Figure 9d are proportional to the difference between the two principal strain rates. Purely strike-slip faulting is expected where the two directions are perpendicular. Dip-slip faulting is expected where the two directions are parallel, otherwise oblique faulting is implied. The fault strikes in Figure 9d provide a check on the consistency between the predicted set of faults that can uniformly accommodate the GPS

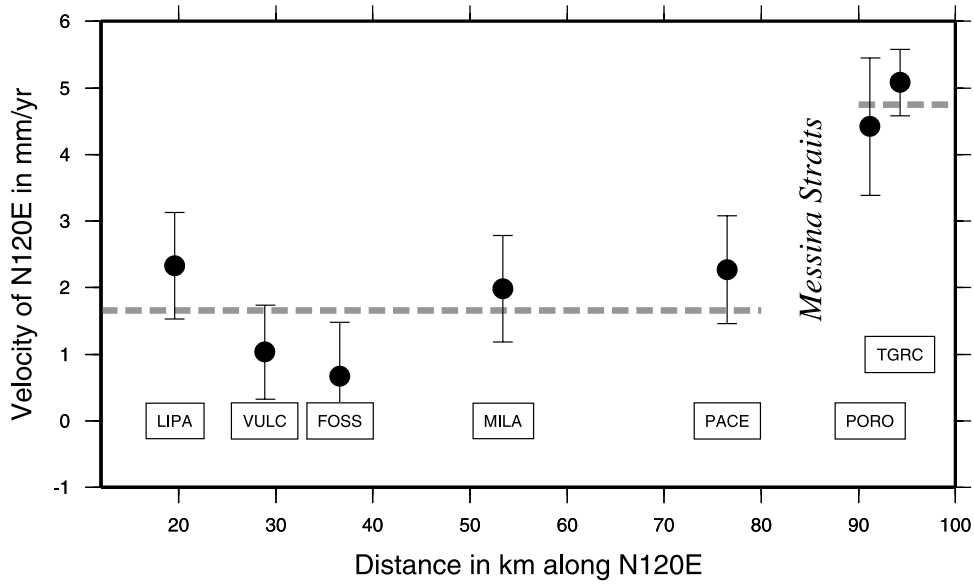

Figure 10. Velocity in the N120°E direction as a function of distance along the same direction. The error bars represent 1 standard deviation. Horizontal thick gray dashed lines mark the N120°E velocities averaged for the sites on the sides of the Messina Straits. Observed GPS velocities are consistent with a ~3 mm/yr increase of velocity and active extension in the Straits.

velocity field and the pattern of faulting shown by geological and seismological data. The predicted strikes are similar to the NW trending right-lateral faulting observed in the Aeolian Islands, and NNE trending normal faults (with a right-lateral component) in the Messina Straits. A remarkable parallelism is observed between one of the predicted directions and the direction of the coast in the Messina Straits, which is probably controlled by faulting [*Valensise and Pantosti*, 1992]. Equation (1) implies that there may be more than one way in which distributed deformation can be accommodated by faulting. The main results of this comparison is that, despite the apparent complexity of the velocity field, one of the predicted set of faults (by which the velocity field can be theoretically accommodated by distributed deformation) is consistent with fault patterns independently observed by the geology and seismology. Furthermore these predictions are indicative of strain accumulation on seismically active faults.

[15] Given the observed and predicted patterns of faulting, the comparison of Figures 9d and 9c suggests that instantaneous rotations are likely to be released by right-lateral slip on NW striking faults in the western part of the analyzed network, so that no secular block rotation is expected. In the eastern part (Messina Straits) the observed pattern of faulting suggests instead that deformation may be associated with rotations of NNE striking normal fault blocks with a right-lateral component of slip. Our results do not support the existence of a single throughgoing NNW trending active faults cutting from the Aeolian Islands to the Malta escarpment, as proposed by *Lanzafame and Bousquet* [1997]. Our results favor the view in which an area of distributed deformation separates the Ionian lithosphere and the Calabrian Arc to the east from the Sicilian block to the west which transmits most of the Nu motion to the E-W trending offshore seismic belt in the Southern Tyrrhenian. The dense GPS network covering the region between Sicily and Calabria allows us to estimate the amount of relative motion between Sicily and the Calabrian Arc taken up in the Messina Straits. The increase in velocity and extension in the Messina Straits are best shown by projecting site velocities (Figure 10) onto a single profile constructed parallel to the estimated relative motion direction. A sudden increase in velocity occurs across the Messina Straits, where localized deformation may accommodate up to 3 mm/yr and approximately 80% of the relative motion estimated in Figure 8.

6. Discussion

6.1. Slip Partitioning in the Calabrian Arc or Independent Ionian Block?

[16] Slip partitioning of the oblique convergence into its orthogonal trench-parallel and trench-perpendicular components is frequently observed in many convergent settings [*Jarrard*, 1986; *DeMets et al.*, 1990]. Figure 11 shows the site velocities along the Calabrian Arc compared with the Eu and Nu-fixed velocities predicted for a complete partitioning of the Eu-Nu convergence. Rather than the poor bathymetric expression of the trench we use the average N20°E trend of the Calabrian Arc as a proxy for the trench direction, corresponding to a 25° obliquity angle between the plate convergence vector and the normal to the trench. The comparison between the observed and predicted velocities provides good evidence for slip partitioning of the oblique Eu-Nu convergence. On the other hand this hypothesis relies on the assumption of the Ionian block as a part of the Nubia plate. An alternative hypothesis, proposed by *Westaway* [1990], suggests the existence of an independent Ionian block, rotating counterclockwise with respect to Nubia and intermediate between such plate and the Adriatic microplate.

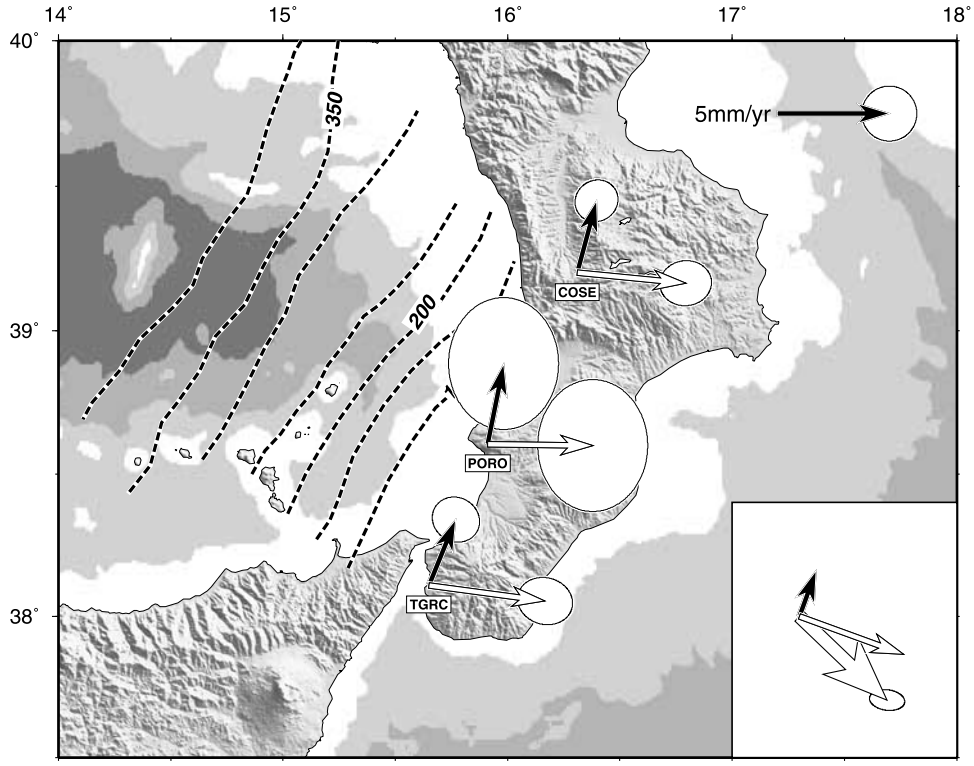

Figure 11. GPS velocity of the Calabrian Arc in a Eurasian (black) and Nubia (white) reference frames. The vectors in the inset represent the calculated slip partitioning of the oblique Nu-Eu convergence (large, white arrow) at 17.3°E, 38.0°N in its trench-parallel (small, black arrow) and trench-perpendicular (small, white arrow) components, taking N20°E as the trench direction.

The pole of rotation of the Ionian block (with respect to Nubia) has been located by *Westaway* [1990] in Libya resulting in normal faulting along the eastern coast of Sicily and oblique extension in Calabria. The lack of islands in the rigid Ionian Sea precludes the use of GPS to test the existence of such block. Further information on the active deformation of the Ionian wedge is thus likely to be provided by seismological data and reflection profiling experiments in the Ionian wedge and densification of the GPS network along the Calabrian Arc.

[17] Active tectonics and seismicity in Calabria are generally attributed to N-S to NE-SW trending active normal faults that dominate the geomorphology and follow the axis of the Calabria peninsula [*Tortorici et al.*, 1995; *Jacques et al.*, 2001; *Galli and Bosi*, 2002, 2003]. Because of the lack of geodetic sites along the eastern side of Calabria, we are not able to detect strain accumulation across these active faults, which may be loaded by increasing southeastward velocities. The NNE directed motion of the TGRC, COSE and PORO sites, predicts that a component of left-lateral motion on north to NNE trending fault should allow transport of the Calabrian Arc toward NNE with respect to the Tyrrhenian Sea and the Sardinia-Corsica block. Over a period of about 250 years (1659–1908) almost the whole active fault system along the Calabrian Arc ruptured through $M \sim 6$–7 earthquakes [*Jacques et al.*, 2001; *Galli and Bosi*, 2002, 2003]. Although the slip vectors of these earthquakes are poorly constrained, significant evidence of left-lateral slip have been observed by *Galli and Bosi* [2003] along the 1683 earthquake fault ruptures.

6.2. Eu-Nu Plate Boundary and Style of Deformation

[18] With respect to the style of Eu-Nu convergence we recognize distinct styles of deformation taking up the shortening in the plate boundary. The southern and western part of Sicily can be kinematically considered as the northernmost edge of the Nubia plate. Geological, seismological and geodetic evidence support the hypothesis that active Eu-Nu convergence has probably shifted from the front of the Plio-Pleistocene nappes to the Southern Tyrrhenian Sea, that previously worked as the transtensional passive margin of the back arc basin [see also *Pondrelli et al.*, 2004]. Site velocities in Calabria suggest that underthrusting of the Ionian lithosphere may still occur, although back arc extension in the Tyrrhenian Sea is no longer active. An explanation for these distinct behaviors probably resides in the different structure of the lithosphere approaching the plate boundary zone, well imaged by the difference in bathymetry across the Malta escarpment (Figure 1). The deep and negatively buoyant Mesozoic oceanic lithosphere [*Catalano et al.*, 2001] can be easily subducted beneath the Calabrian Arc. The lack of evidence for active spreading, when compared with Neogene-Quaternary estimates of 50–70 mm/yr of back arc extension, is indicative of a substantial recent deceleration of the rollback of the Ionian lithosphere. The reason for the rollback slowing down is not clear but one can speculate that the episodic nature of back

arc extension, the interaction with the 670 km discontinuity or the progressive narrowing of the incoming oceanic lithosphere may have been responsible for rollback deceleration [*Faccenna et al.*, 2001b]. The continental nature and the progressive buoyancy of the lithosphere approaching the subduction front in Sicily, together with the resistance exerted by the rigid Hyblean block, may have induced the Eu-Nu convergence to jump north of Sicily in the Southern Tyrrhenian zone. In this area the contrast in elevation with the low-lying Tyrrhenian basin and the preexisting structures may have favored the concentration of deformation taking up the Eu-Nu convergence. We observe that this pattern is common to other regions along the Eurasia-Nubia plate boundary, such as the northern African coast where active convergence is currently taken up along the former Neogene passive margin separating the Algero-Provencal basin in the north from the Tell and Atlas thrust and fold belt to the south [*Morel and Meghraoui*, 1996]. To the first-order, the style of Eu-Nu convergence in western Sicily does not require intermediate crustal blocks or widely distributed deformation, since the earthquake slip vectors in the Southern Tyrrhenian zone may directly reflect the Eu-Nu relative kinematics. An additional intermediate crustal block, that can be interpreted in terms of slip partitioning of the oblique convergence in the Calabrian Arc or as an independent Ionian block, is instead required by GPS data in Calabria. Following the first interpretation we speculate that the oblique convergence forces the Calabrian sliver to move semirigidly toward NE with respect to Eurasia, inducing extension at its trailing edge in the Messina Straits. We also speculate that deceleration of slab roll-back may have forced slip partitioning in the overlying forearc, producing NNE motion of the Calabrian Arc and rifting in the Messina Straits, cutting at high angle across the preexisting thrust structures [*Monaco et al.*, 1996]. Stratigraphical constraints on the initiation of rifting in the Messina Straits may provide important data to verify this hypothesis.

[19] Strain analysis and style of faulting show that NW-SE right-lateral shear in the Aeolian Islands and extension in the Messina Straits dominate the tectonic regime between Sicily and the Calabrian Arc. These observations, however, do not explain the NE motion of the Sicilian corner away from its mainland, perpendicularly to the Eu-Nu convergence vector. This motion is consistent with normal-faulting low-magnitude earthquakes in northeastern Sicily, with NE-SW directed extension direction [*Pondrelli et al.*, 2004]. A first hypothesis may include the lateral extrusion and sideways expulsion perpendicular to the relative plate motion, of the northeastern part of Sicily away from the collision zone. We also speculate that others possible mechanisms may also include the perturbing effects exerted by the mantle anomaly beneath the Etna volcano on crustal motion. Mantle upwelling beneath eastern Sicily has been suggested to explain the intense magmatism and the evolution of the Etna volcano [*Tanguy et al.*, 1997], and has been proposed from seismic tomography analyses [*Montelli et al.*, 2004].

[20] Geological data [*Bordoni and Valensise*, 1998] show that the 125 kyr shorelines (stage 5e of the oxygen isotopic scale commonly called "Tyrrhenian") is regionally uplifted in an area centered over the Messina Straits with elevations decreasing radially away from eastern Sicily and the Etna volcano. Since no evidence support active crustal thickening and magmatic underplating which may have contributed to isostatically raise the surface, and seismic evidence point for a shallower Moho beneath Etna [*Nicolich et al.*, 2000], we speculate that the recent uplift in eastern Sicily may be of dynamic origin and related to mantle upwelling at the western edge of the Ionian slab. Convective flow in the mantle produces vertical deformation of the surface induced by the normal stresses applied at the base of the lithosphere. This dynamic uplift may have increased the gravitational potential energy of the elevated region. The most favorable direction in which the gradient of potential energy is likely to drive deformation is perpendicular to the convergence vector and away from the rigid Sicilian block. Our hypothesis thus emphasizes a combination of factors related to the kinematics and geometry of the Eu-Nu boundary and to the contribution of upper mantle dynamics to crustal motion. The understanding of the relative importance of these factors is currently difficult to evaluate and will require additional seismic and geodetic information on the upper mantle structure and the crustal velocity field.

6.3. Implications for Seismic Hazard

[21] Our results suggest that up to 80% of the 3.6 ± 0.6 mm/yr relative motion between the Sicilian and Calabrian blocks may be absorbed in the Messina Straits loading the fault responsible for the 1908 M_w 7.1 earthquake. Geological estimates of horizontal slip rate along the Messina fault of about 1 mm/yr [*Valensise and Pantosti*, 1992] may indicate that (1) a significant deformation occurs by aseismic slip, (2) other faults are required to accommodate this relative motion, or (3) biases in the geological and/or geodetic estimates. Beyond the 1908 Messina seismic event large historical earthquakes are documented in eastern Sicily, such as the devastating 1693 earthquakes [*Boschi et al.*, 1995], whose fault geometry and location is still a matter of debate [*Bianca et al.*, 1999; *Piatanesi and Tinti*, 1998]. Our kinematic reconstruction allows us to recognize two possible mechanisms for large earthquakes in this region. The first is the ESE motion of the Calabrian Arc with respect to Sicily. We consider this motion responsible for active extension in the Messina Straits and expect it to extend south of the Straits inducing extensional strain along the eastern coast of Sicily [*Monaco et al.*, 1997]. The other mechanism is the progressive tearing of the subducting Ionian oceanic lithosphere from the adjacent continental lithosphere in the Hyblean Plateau [*Doglioni et al.*, 2001]. Seismic reflection lines in the Ionian Sea offshore eastern Sicily [*Argnani et al.*, 2002] show that the fault system forming the Malta escarpment is frequently associated with deformation of recent sediments and disruption of the ocean floor, suggesting the possible reactivation of this structure during catastrophic earthquakes such as the large 1693 seismic event. GPS velocities in eastern Sicily are consistent with low strain rates across the area of the M_w 5.9 1968 Belice earthquake (between NOTO and TRAP-MILO) and higher strain rates north of Sicily where most of the Eu-Nu convergence seems to be accommodated. An important issue for seismic hazard assessment is connected to the mode of seismic release of the Eu-Nu shortening taken up

in north of Sicily and in the Ionian wedge where rates of 4–5 mm/yr have been estimated. Given the low-level of the seismic deformation in northern Sicily and in the Ionian Sea, a considerable deficit of seismic release is found in both areas, which can be released in future events.

7. Conclusion

[22] The results of this work suggest that two different styles of deformation accommodate the Eurasia-Nubia convergence in Sicily and in the Calabrian Arc. In Sicily geodetic and seismological evidence suggest that 4–5 mm/yr of Eu-Nu convergence are principally accommodated to the north in the Southern Tyrrhenian zone with recent cessation of outward (south) motion of the thrust sheets along the Plio-Pleistocene subduction front. In the Calabrian Arc residual velocities with respect to both the Eurasia and Nubia plates are consistent with the presence of a forearc sliver in the Calabrian Arc partitioning 5 mm/yr of oblique convergence in 2 mm/yr of trench-parallel and 3 mm/yr of trench-perpendicular velocities. An area of diffused deformation, which includes the northeastern corner of Sicily, the Aeolian Islands and the Messina Straits, accommodates the relative motion between Sicily and the Calabrian Arc by right-lateral shear, normal faulting and clockwise rotations. We show that (1) available information on the source geometry of the M_w 7.1 1908 Messina earthquake are compatible with the accommodation of this relative motion and that (2) up to 3 mm/yr (80% of the relative motion) can be taken up in the Messina Straits. Statistically insignificant elongation of the baselines crossing the Tyrrhenian Sea do not support active back arc spreading consistently with the low level of crustal seismicity in the Tyrrhenian basin. The alternative hypothesis of an independent Ionian block, intermediate between the Nubia plate and the Adriatic block is currently difficult to be tested, and awaits further information to be evaluated.

[23] We suggest that the different style of deformation along the plate boundary are caused by the different lithospheric structures: the Mesozoic oceanic lithosphere may still be subducted beneath the Calabrian Arc or behaving as an independent Ionian block, whereas the continental lithosphere approaching the plate boundary in Sicily resists subduction and transmits the Nubia motion to the Southern Tyrrhenian zone where most of the convergence is accommodated. Future geodetic studies and densification of the permanent network are needed to provide information on specific topics of the active deformation that have significant implications for the seismic hazard. One of these topics is the understanding of the mode of active shortening in those regions (such as the Ionian wedge and the Southern Tyrrhenian zone) that, presenting a significant deficit of the seismic release, may potentially accommodate part of the convergence by aseismic creep or slow deformation.

[24] **Acknowledgments.** We thank the following institutions for facilitating the availability of GPS data: ASI (http://geodaf.mt.asi.it), SOPAC (http://sopac.ucsd.edu), UNAVCO (http://www.unavco.org) and EUREF (http://www.epncb.oma.be). We also thank Giuseppe Casula, Pino Colucci, Salvatore Gabriele, Alessandro Galvani, Enzo Mantovani and Marco Mucciarelli for Rinex data. N.D. acknowledges the Fulbright Commission for fellowship support at the Jet Propulsion Laboratory in Pasadena in 2000–2001. Fruitful discussions with James Jackson, Stefano Sylos Labini, Fabrizio Antonioli, and Gianluca Valensise have been found useful. We also thank the Associate Editor Yehuda Bock and the reviewers Rob Reilinger and Shimon Wdowinski for useful comments and criticisms. This work is partially funded by the Civil Protection GNDT project "Probable earthquakes in Italy between the year 2000 and 2030: guidelines for determining priorities in risk mitigation". Figures were produced using GMT version 3.4.

References

Amoruso, A., L. Crescentini, and R. Scarpa (2002), Source parameters of the 1908 Messina Straits, Italy, earthquake from geodetic and seismic data, *J. Geophys. Res.*, *107*(B4), 2080, doi:10.1029/2001JB000434.

Anderson, H., and J. A. Jackson (1987), Active tectonics in the Adriatic region, *Geophys. J. R. Astron. Soc.*, *91*, 937–983.

Anzidei, M., P. Baldi, C. Bonini, G. Casula, S. Gandolfi, and F. Riguzzi (1998), Geodetic surveys across the Messina Straits (southern Italy) seismogenetic area, *J. Geodyn.*, *25*(2), 85–97.

Anzidei, M., P. Baldi, G. Casula, A. Galvani, E. Mantovani, A. Pesci, F. Riguzzi, and E. Serpelloni (2001), Insights into present-day crustal motion in the central Mediterranean area from GPS surveys, *Geophys. J. Int.*, *146*, 98–110.

Argnani, A., et al. (2002), Tectonics of eastern Sicily offshore: Preliminary results from the MESC 2001 marine seismic cruise, *Boll. Geofis. Teor. Appl.*, *43*(3–4), 177–193.

Argus, D. F., R. G. Gordon, C. DeMets, and S. Stein (1989), Closure of the Africa-Eurasia-North American plate motion circuit and tectonics of the Gloria fault, *J. Geophys. Res.*, *94*, 5585–5602.

Battaglia, M., M. H. Murray, E. Serpelloni, and R. Bürgmann (2004), The Adriatic region: An independent microplate within the Africa-Eurasia collision zone, *Geophys. Res. Lett.*, *31*, L09605, doi:10.1029/2004GL019723.

Bianca, M., C. Monaco, L. Tortorici, and L. Cernobori (1999), Quaternary normal faulting in southeastern Sicily (Italy): A seismic source for the 1693 earthquake, *Geophys. J. Int.*, *139*, 370–394.

Blewitt, G., and D. Lavallée (2002), Effect of annual signals on geodetic velocity, *J. Geophys. Res.*, *107*(B7), 2145, doi:10.1029/2001JB000570.

Bonaccorso, A. (2002), Ground deformation of the southern sector of the Aeolian Islands volcanic arc from geodetic data, *Tectonophysics*, *351*, 181–192.

Bordoni, P., and G. Valensise (1998), Deformation of the 125ka marine terrace in Italy: Tectonic implications, in *Coastal Tectonics*, edited by I. S. Stewart and C. Vita-Finzi, *Geol. Soc. Spec. Publ.*, *146*, 71–110.

Boschi, E., D. Pantosti, and G. Valensise (1989), Modello di sorgente per il terremoto di Messina del 1908 ed evoluzione recente dell'area dello stretto, paper presented at Atti 89th GNDT Workshop, Cons. Naz. delle Ric., Rome.

Boschi, E., G. Ferrari, P. Gasperini, E. Guidoboni, G. Smriglio, and G. Valensise (1995), Catalogo Dei Forti Terremoti in Italia Dal 461 A. C. Al 1980, Ist. Naz. di Geofis., Rome.

Butler, R. W. H., M. Grasso, and F. La Manna (1992), Origin and deformation of the Neogene-Recent Maghrebian foredeep at the Gela Nappe, SE Sicily, *J. Geol. Soc. London*, *149*, 547–556.

Calais, E., J. M. Nocquet, F. Jouanne, and M. Tardy (2002), Current extension in the central part of the Western Alps from continuous GPS measurements, 1996–2001, *Geology*, *30*, 651–654.

Calais, E., C. DeMets, and M. Nocquet (2003), Evidence for a post-3.16-Ma change in Nubia-Eurasia-North America plate motions?, *Earth Planet. Sci. Lett.*, *216*, 81–92.

Catalano, R., C. Doglioni, and S. Merlini (2001), On the Mesozoic Ionian Basin, *Geophys. J. Int.*, *144*, 49–64.

Chiarabba, C., L. Jovane, and R. Di Stefano (2004), Instrumental seismicity and seismotectonics of Italy, *Tectonophysics*, in press.

DeMets, C., R. G. Gordon, D. F. Argus, and S. Stein (1990), Current plate motions, *Geophys. J. Int.*, *101*, 425–478.

DeMets, C., R. G. Gordon, D. F. Argus, and S. Stein (1994), Effect of recent revisions to the geomagnetic reversals time scale on estimates of current plate motions, *Geophys. Res. Lett.*, *21*, 2191–2194.

Dixon, T. H., M. Miller, F. Farina, H. Wang, and D. Johnson (2000), Present-day motion of the Sierra Nevada block and some tectonic implications for the Basin and Range province, North American Cordillera, *Tectonics*, *19*, 1–24.

Doglioni, C., F. Innocenti, and G. Mariotti (2001), Why Mt Etna?, *Terra Nova*, *13*, 25–31.

Engdahl, E. R., R. van der Hilst, and R. Buland (1998), Global teleseismic earthquake relocation with improved travel times and procedures for depth determination, *Bull. Seismol. Soc. Am.*, *88*, 722–743.

Faccenna, C., T. W. Becker, F. P. Lucente, L. Jolivet, and F. Rossetti (2001a), History of subduction and back-arc extension in the central Mediterranean, *Geophys. J. Int.*, *145*, 809–820.

Faccenna, C., F. Funiciello, D. Giardini, and F. P. Lucente (2001b), Episodic back-arc extension during restricted mantle convection in the central Mediterranean, *Earth Planet. Sci. Lett.*, *87*, 105–116.

Fernandes, R. M. S., B. A. C. Ambrosius, and R. Noomen (2003), The relative motion between Africa and Eurasia as derived from ITRF2000 and GPS data, *Geophys. Res. Lett.*, *30*(16), 1828, doi:10.1029/2003GL017089.

Frepoli, A., G. Selvaggi, C. Chiarabba, and A. Amato (1996), State of stress in the Southern Tyrrhenian subduction zone from fault-plane solutions, *Geophys. J. Int.*, *125*, 879–891.

Galli, P., and V. Bosi (2002), Paleoseismology along the Cittanova fault: Implications for seismotectonics and earthquake recurrence in Calabria (southern Italy), *J. Geophys. Res.*, *107*(B3), 2044, doi:10.1029/2001JB000234.

Galli, P., and V. Bosi (2003), Catastrophic 1638 earthquakes in Calabria (southern Italy): New insights from paleoseismological investigation, *J. Geophys. Res.*, *108*(B1), 2004, doi:10.1029/2001JB001713.

Gvirtzman, Z., and A. Nur (1999), The formation of Mount Etna as the consequence of slab rollback, *Nature*, *401*, 782–785.

Hollenstein, C. H., H.-G. Kahle, A. Geiger, S. Jenny, S. Goes, and D. Giardini (2003), New GPS constraints on the Africa-Eurasia plate boundary zone in southern Italy, *Geophys. Res. Lett.*, *30*(18), 1935, doi:10.1029/2003GL017554.

Holt, W. E., and A. J. Haines (1993), Velocity fields in deforming Asia from the inversion of earthquake-released strains, *Tectonics*, *12*, 1–20.

Hunstad, I., G. Selvaggi, N. D. Agostino, P. England, P. Clarke, and M. Pierozzi (2003), Geodetic strain in peninsular Italy between 1875 and 2001, *Geophys. Res. Lett.*, *30*(4), 1181, doi:10.1029/2002GL016447.

Jacques, E., C. Monaco, P. Tapponnier, L. Tortorici, and T. Winter (2001), Faulting amd earthquake triggering during the 1783 calabria seismic sequence, *Geophys. J. Int.*, *147*, 499–516.

Jarrard, R. D. (1986), Relations among subduction parameters, *Rev. Geophys.*, *24*, 217–284.

Lanzafame, G., and J. C. Bousquet (1997), The Maltese escarpment and its extension from Mt. Etna to the Aeolian Islands (Sicily): Importance and evolution of a lithosphere discontinuity, *Acta Vulcanol.*, *9*, 113–120.

Malinverno, A., and W. B. Ryan (1986), Extension in the Tyrrhenian Sea and shortening in the Apennines as arc migration driven by the sinking of the lithosphere, *Tectonics*, *5*, 227–245.

Mao, A., C. G. A. Harrison, and T. H. Dixon (1999), Noise in GPS coordinate time series, *J. Geophys. Res.*, *104*, 2797–2816.

Marani, M. P., and T. Trua (2002), Thermal constriction and slab tearing at the origin of a superinflated spreading ridge: Marsili volcano (Tyrrhenian Sea), *J. Geophys. Res.*, *107*(B9), 2188, doi:10.1029/2001JB000285.

Mazzuoli, R., L. Tortorici, and G. Ventura (1995), Oblique rifting in the Aeolian Islands, *Terra Nova*, *7*, 444–452.

McClusky, S., R. Reilinger, S. Mahmoud, D. Ben Sari, and A. Tealeb (2003), GPS constraints on Africa (Nubia) and Arabia plate motions, *Geophys. J. Int.*, *155*, 126–138.

McKenzie, D. (1972), Active tectonics of the Mediterranean region, *Geophys. J. R. Astron. Soc.*, *30*, 109–185.

Monaco, C., L. Tortorici, R. Nicolich, L. Cernobori, and M. Costa (1996), From collisional to rifted basins, an example from the southern Calabrian Arc (Italy), *Tectonophysics*, *266*, 233–249.

Monaco, C., P. Tapponnier, L. Tortorici, and P. Y. Gillot (1997), Late Quaternary slip rates on the Acireale-Piedimonte normal faults and tectonic origin of Mt. Etna (Sicily), *Earth Planet. Sci. Lett.*, *147*, 125–139.

Montelli, , G. Nolet, F. A. Dahlen, G. Masters, E. R. Engdahl, and S. Hung (2004), Finite-frequency tomography reveals a variety of plumes in the mantle, *Science*, *303*, 338–343.

Morel, J. L., and M. Meghraoui (1996), Goringe-Alboran-Tell tectonic zone: A transpression system along the Africa-Eurasia plate boundary, *Geology*, *24*, 755–758.

Nicolich, R., M. Laigle, A. Hirn, L. Cernobori, and J. Gallart (2000), Crustal structure of the Ionian margin of Sicily: Etna volcano in the frame of regional evolution, *Tectonophysics*, *329*, 121–139.

Oldow, J. S., L. Ferranti, D. S. Lewis, J. K. Campbell, B. D'Argenio, R. Catalano, G. Pappone, L. Carmignani, P. Conti, and C. L. V. Aiken (2002), Active fragmentation of Adria, the north African promontory, central Mediterranean orogen, *Geology*, *30*, 779–782.

Patacca, E., R. Sartori, and P. Scandone (1990), Tyrrhenian basin and Apenninic arcs. Kinematic relations since late Tortonian times, *Mem. Soc. Geol. Ital.*, *45*, 425–451.

Pepe, F., G. Bertotti, F. Cella, and E. Marsella (2000), Rifted margin formation in the south Tyrrhenian Sea: A high-resolution seismic profile across the north Sicily passive continental margin, *Tectonics*, *19*, 241–257.

Piatanesi, A., and S. Tinti (1998), A revision of the 1693 eastern Sicily earthquake and tsunami, *J. Geophys. Res.*, *103*, 2749–2758.

Pino, A. N., D. Giardini, and E. Boschi (2000), The December 28, 1908, Messina Straits, southern Italy, earthquake: Waveform modeling of regional seismograms, *J. Geophys. Res.*, *105*, 25,473–25,492.

Pondrelli, S., C. Piromallo, and E. Serpelloni (2004), Convergence vs. retreat in Southern Tyrrhenian Sea: Insights from kinematics, *Geophys. Res. Lett.*, *31*, L06611, doi:10.1029/2003GL019223.

Sella, G., T. H. Dixon, and A. Mao (2002), REVEL: A model for Recent plate velocities from space geodesy, *J. Geophys. Res.*, *107*(B4), 2081, doi:10.1029/2000JB000033.

Selvaggi, G. (2001), Strain pattern of the Southern Tyrrhenian slab from moment tensors of deep earthquakes: Implications on the down-dip velocity, *Ann. Geofis.*, *44*(1), 155–165.

Selvaggi, G., and C. Chiarabba (1995), Seismicity and *P*-wave velocity image of the Southern Tyrrhenian subduction zone, *Geophys. J. Int.*, *121*, 818–826.

Shen, Z. K., D. D. Jackson, and B. X. Ge (1996), Crustal deformation across and beyond the Los Angeles basin from geodetic measurements, *J. Geophys. Res.*, *101*, 27,957–27,980.

Tanguy, J. C., M. Condomines, and G. Kieffer (1997), Evolution of the Mount Etna magma: constraints on the present feeding system and eruptive mechanism, *J. Volcanol. Geotherm. Res.*, *75*, 221–250.

Torelli, L., M. Grasso, G. Mazzoldi, and D. Peis (1998), Plio-Quaternary tectonic evolution and structure of the Catania foredeep, the northern Hyblean Plateau and the Ionian shelf (SE Sicily), *Tectonophysics*, *298*, 209–221.

Tortorici, L., C. Monaco, C. Tansi, and O. Cocina (1995), Recent and active tectonics in the Calabrian Arc (southern Italy), *Tectonophysics*, *243*, 37–55.

Valensise, G., and D. Pantosti (1992), A 125 Kyr-long geological record of seismic source repeatibility: The Messina Straits (southern Italy) and the 1908 earthquake (M_S 7 $^1/_2$), *Terra Nova*, *4*, 472–483.

Ward, S. N. (1994), Constraints on the seismotectonics of the central Mediterranean from very long-base-line interferometry, *Geophys. J. Int.*, *117*, 441–452.

Westaway, R. (1990), Present-day kinematics of the plate boundary zone between Africa and Europe, from the Azores to the Aegean, *Earth Planet. Sci. Lett.*, *96*, 393–406.

Zumberge, J. F., M. B. Heflin, D. C. Jefferson, M. M. Watkins, and J. F. H. Webb (1997), Precise point positioning for the efficient and robust analysis of GPS data from large networks, *J. Geophys. Res.*, *102*, 5005–5017.

N. D'Agostino and G. Selvaggi, Istituto Nazionale di Geofisica e Vulcanologia, Via di Vigna Murata, 605, I-00143 Rome, Italy. (dagostino@ingv.it)